



# Individual exposure estimates may be erroneous when spatiotemporal variability of air pollution and human mobility are ignored



Yoo Min Park, Mei-Po Kwan\*

Department of Geography and Geographic Information Science, University of Illinois at Urbana-Champaign, Champaign, IL 61820, USA

## ARTICLE INFO

### Keywords:

Environmental health  
Air pollution exposure  
Human mobility  
The uncertain geographic context problem (UGCoP)  
3D geovisualization

## ABSTRACT

This study aims to empirically demonstrate the necessity to consider both the spatiotemporal variability of air pollution and individual daily movement patterns in exposure and health risk assessment. It compares four different types of exposure estimates generated by using (1) individual movement data and hourly air pollution concentrations; (2) individual movement data and daily average air pollution data; (3) residential location and hourly pollution levels; and (4) residential location and daily average pollution data. These four estimates are significantly different, which supports the argument that ignoring the spatiotemporal variability of environmental risk factors and human mobility may lead to misleading results in exposure assessment. Additionally, three-dimensional (3D) geovisualization presented in the paper shows how person-specific space-time context is generated by the interactions between air pollution and an individual, and how the different individualized contexts place individuals at different levels of health risk.

## 1. Introduction

Air pollution can lead to a variety of health problems, such as respiratory and cardiovascular issues, lung cancer, and even premature death. The American Lung Association reports that ground-level ozone is the most widespread pollutant in the U.S., and it is especially harmful to children, the elderly, people with cardiovascular or lung diseases, and people who work outdoors. To better assess the adverse health effects of ozone on humans, it is important to estimate personal exposure more accurately. Given that the level of air pollution is continuously changing over space and time and that humans are mobile across space, both of these dynamic characteristics and their complex interactions should be considered in order to accurately assess personal exposure levels (Buonanno et al., 2014; Dons et al., 2011; Fang and Lu, 2012; Kwan et al., 2015; Lu and Fang, 2015; Pilla and Broderick, 2015; Ryan et al., 2015; Steinle et al., 2013, 2015; Yoo et al., 2015; Zhou et al., 2011).

However, many previous environmental health/exposure studies tended to assume that air pollution levels are spatially stationary and temporally constant throughout a day, month, or year or that people are non-mobile and thus are not exposed to air pollution in areas outside of their residential neighborhoods. For example, one study used a ten-year geometric mean concentration of ambient air pollution and census-tract level socioeconomic and demographic data (Jerrett et al., 2001). Similarly, Gray et al. (2013) utilized daily average

particulate matter (PM<sub>2.5</sub>) concentrations, daily eight-hour maximum ozone concentrations, and census-tract level demographic data. In Buzzelli and Jerrett (2007)'s study, the two-week average of nitrogen dioxide (NO<sub>2</sub>) concentrations in Toronto was used together with Statistics Canada's 2001 census data to obtain the socioeconomic status of places of residence. Some other studies attempted to take human mobility and non-residential exposures into account (Chum and O'Campo, 2013; Nyhan et al., 2016; Setton et al., 2008). However, these studies also used temporally aggregated air pollution data (the average weekday 24-h traffic volume data as a proxy for air pollution; daily PM<sub>2.5</sub> concentrations; and the annual average NO<sub>2</sub> concentrations, respectively).

While these previous studies offer a useful foundation for future research, they have several limitations. First, because air pollution levels not only change across space but also change between hours or even minutes, it is important to consider their spatiotemporal variations and the dynamic interactions between pollutants and humans at fine spatiotemporal scales (Yoo et al., 2015). In reality, people are not affected by the "average" pollution level but by specific hourly pollution levels during a day, which can directly cause acute symptoms (e.g., acute asthma). Therefore, hourly air pollution concentrations seem more relevant to vulnerable people than merely the daily or monthly average, because finer temporal information would enable them to change their daily space-time behaviors to minimize exposure.

Second, it has been noted that personal or individual exposure to

\* Corresponding author.

E-mail addresses: [ypark96@illinois.edu](mailto:ypark96@illinois.edu) (Y.M. Park), [mpk654@gmail.com](mailto:mpk654@gmail.com) (M.-P. Kwan).

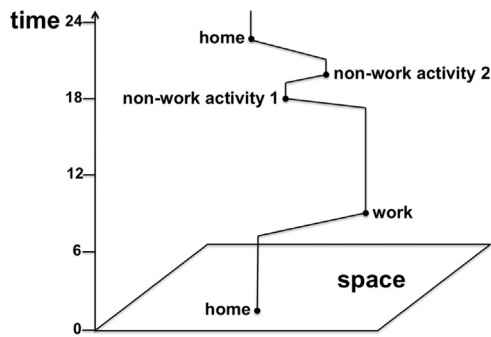


**Fig. 1.** An individual's daily movement trajectory can be represented as a continuous temporal sequence from the time-geographic perspective. Time geography was originally developed by Hägerstrand (1970), and it provides a useful framework for examining the complex interaction between human movement and environmental stressors in space-time.

environmental influences is determined both by a person's specific location and how much time the person spends there when undertaking daily activities—such as work, grocery shopping, and other non-work activities (see Fig. 1)—rather than being determined solely by the person's residential area (Crawford et al., 2014; de Nazelle et al., 2013; Kwan, 2009, 2012a; Kwan et al., 2015; Setton et al., 2011; Yoo et al., 2015). This means that *where people live* is often not the only important factor in determining their exposure to environmental factors. Rather, *where people visit* and *how much time they spend at a particular location* are more relevant to assessing the effects of environmental factors on people's health behaviors or outcomes. Since most previous studies did not take into account the variety of places that people visit on a daily basis (Hernandez et al., 2015), they did not capture the full range of personal exposure at various locations and moments.

These two underlying assumptions often found in previous environmental health studies may lead to considerable uncertainty in research results, as part of the uncertain geographic context problem (UGCoP) (Kwan, 2012a,b) that has recently been articulated. The UGCoP refers to the issue that research conclusions about the effects of environmental influences on a person's health are sensitive to different delineations of the geographic and temporal contexts used to derive the relevant environmental variables. This problem arises when data are aggregated over areas (e.g., census tracts) that do not necessarily correspond to where people actually visit in their daily lives and have a coarse temporal resolution, because such data contain uncertainties in the relevant spatiotemporal contexts in which an individual is exposed to environmental influences, such as air pollution (Kwan, 2012a). As a result, findings from studies that are based on either of these two assumptions may be inaccurate or even entail a significant inferential error.

Since the UGCoP may contribute to misleading findings in studies on environmental (or contextual) effects on people's health behaviors or outcomes (Chen and Kwan, 2015; Kwan, 2012a), some recent studies have begun to pay attention to the UGCoP as a fundamental methodological issue and recognized the need for mitigating its effects on research findings (Liao et al., 2014; Park and Kim, 2014; Robinson and Oreskovic, 2013; Weaver, 2014). Using detailed individual movement data containing accurate spatial and temporal information can mitigate this problem because the data help to delineate the individualized space-time context in which a person is actually affected by relevant environmental or neighborhood factors (Kwan, 2012a,b). In addition, if a relevant environmental factor (i.e., air pollution) continuously changes over space and time at a fine scale, considering the fine spatiotemporal variation of the factor within the individualized space-time context significantly contributes to mitigating the UGCoP as well.

Despite its importance, however, most environmental health stu-

dies to date have paid little attention to the confounding effects of the UGCoP, especially in empirical research on air pollution exposure and its health effects. This may be due to the limited availability of public data, the cost and time for collecting high-resolution data, privacy and data confidentiality issues, and computational complexities (Kwan, 2012b). However, issues regarding personal privacy and cost in this kind of research can be addressed with suitable protective human subjects protocols and adequate funding support. As an alternative, researchers may conduct simulations to create realistic individual-level data based on aggregate data that are widely and publicly available (which is known as “down-scaling” in spatial analysis, and the technique has received increasing attention recently). In addition, recent advances in geographic information science (GIS), geospatial technologies, and geographic masking methods for privacy protection have also helped to address some of these issues (Kwan et al., 2004; Kwan and Schuurman, 2004; Kwan, 2012b). Mobile tracking and sensing technologies (e.g., global positioning systems [GPS] and portable air pollution sensors) have increasingly been used to collect accurate high-resolution data about individual movement and personal exposure to air pollution, which in turn may help address the UGCoP.

As an example of studies using such technology, Lu and Fang (2015) used a GPS-equipped mobile air sensor to collect air pollution levels in a single person's immediate surroundings and presented the movement trajectory using a space-time cube. The mobile sensor enabled them to simultaneously consider real-time air pollution concentrations and human movement patterns. However, because the study used only one person's data, it did not provide adequate empirical evidence for evaluating the argument that multiple people living in the same residential area can experience significantly different exposure levels if they have different movement patterns. Further, although the study visualized a single movement trajectory that was color-coded based on the values of the air quality index, the geovisualization did not include spatiotemporally varying air pollution prediction surfaces simultaneously. Therefore, it is difficult to discern at a glance how the complex interactions between constantly changing spatiotemporal contexts (i.e., the space-time patterns of air pollution) and human movements lead to various exposure levels and potential health effects.

In this study, using geospatial methods and three-dimensional (3D) geovisualization, we aim to empirically demonstrate why including *both* the spatiotemporal dynamics of air pollution and human movement is important in environmental exposure (or health risk) assessments. We argue that the two common assumptions often used in past studies may lead to a considerable inferential error or misleading findings due to the UGCoP. To support this argument, this study compares four different types of exposure estimates generated using four types of data: Simulated individual-level movement patterns, individuals' residential locations, hourly air pollution levels, and daily average pollution levels. In addition, this study uses 3D geovisualization to illustrate how air pollution levels are spatiotemporally dynamic, how people move around during a day, and how potential health effects may vary depending on both of these dynamic patterns during a day. Although this study focuses on Los Angeles County in California, the methods used in the study are also applicable to other cities (in the U.S. or in other countries, such as Canada, Europe, and Asia) where air pollution is a serious health hazard.

## 2. Data and methods

### 2.1. Study area

Los Angeles (LA) County in California, the study area, is well known for having air pollution in the form of smog, which mainly consists of ozone (Gorai et al., 2015). The American Lung Association reports that the Los Angeles-Long Beach metropolitan area in California ranks first for high ozone days among the 277 metropolitan areas in the U.S. The

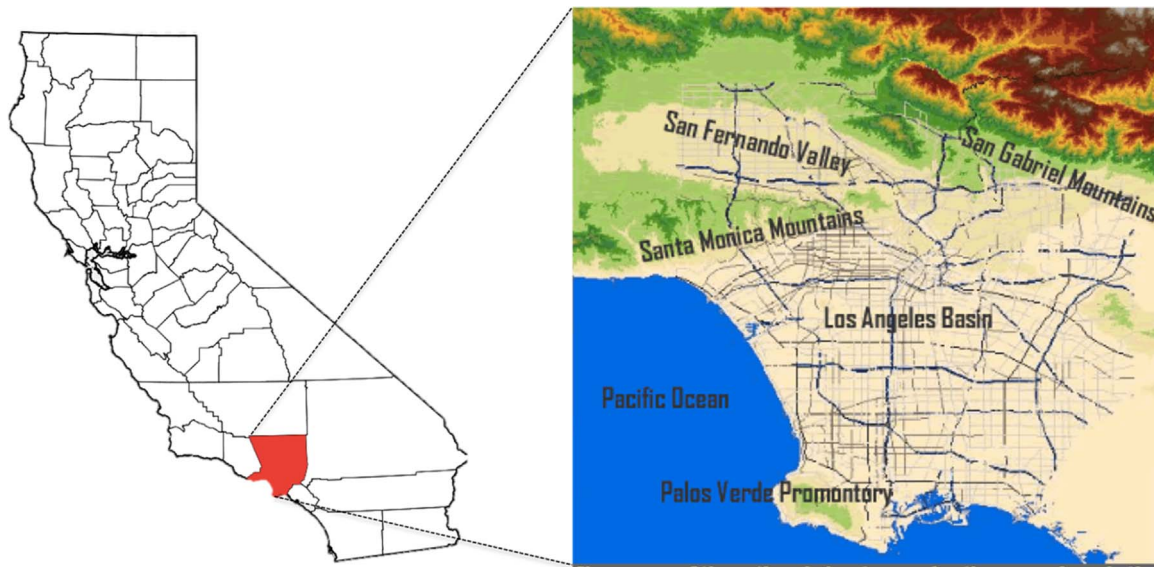


Fig. 2. Study area: Los Angeles County in California.

high levels of ground-level ozone concentration may result from high levels of automobile use and manufacturing activities in the county, because nitrogen oxides (NOx) and volatile organic compounds (VOCs) that contribute to the formation of ground-level ozone come from those mobile and stationary sources (US EPA, 1993), although VOCs also come from natural sources (Bell and Ellis, 2004). In addition, the Los Angeles Basin and the San Fernando Valley easily collect and hold air pollutants. Because of the area's diverse geography, however, air quality across the county is quite heterogeneous. The southern west side and northern east side have different levels of air pollution, because the San Gabriel Mountains run west to east across the county (Fig. 2). This trait of LA County facilitates the identification of the spatial heterogeneity of air pollution and differences in the levels of exposure between individuals who have different space-time movement patterns.

## 2.2. Data

### 2.2.1. Data for geostatistical interpolation (Cokriging)

Cokriging, which is one of the most accurate geostatistical methods that uses secondary variables to increase spatial accuracy, is used to estimate hourly ozone concentrations with two secondary variables: Hourly NOx and hourly temperature data. Monitored hourly ozone and hourly NOx data for 2014 were obtained from the United States Environmental Protection Agency (US EPA), and hourly temperature data were obtained from the California EPA. Although ozone concentrations are higher in the summer than in the winter due to the influence of high temperatures (US EPA, 1993), hourly data in the summer are available from fewer monitoring sites in the US EPA AirData website. Therefore, this study uses data measured on February 23, 2014, which was arbitrarily selected from the winter days with data available from the maximum number of monitoring sites. Data obtained from monitoring sites located in other areas surrounding LA County are also used in order to obtain better estimates of air pollution levels in the study area.

### 2.2.2. Simulated daily movement data

This study simulates 80 possible daily movement trajectories using JavaScript and the Google Maps Directions Service. Possible daily activity locations (e.g., home and work) are chosen based on the daily trip distribution data from the 2010 Congestion Management Program Report (Los Angeles County Metropolitan Transportation Authority, 2010) in order to reflect the actual commuting tendency of LA County

residents.

The report provides commuting pattern information that shows the flow of people across LA County. In the report, census tracts within the Southern California Association of Governments' area are aggregated into Regional Statistical Areas (RSAs) (see Table 1 and Fig. 3). The report provides the percentage of work trips and non-work trips within each RSA and from one RSA to another. We sample these aggregate data as follows (these steps are based on the availability of high-quality demographic data): (1) We sample employer zip codes in LA County by weighting based on the number of employees within each zip code, with this information obtained from the County Business Patterns 2013 data (Bureau of the Census, 2015). (2) After identifying the corresponding RSA for the sampled employer zip code, we determine the RSA of the employees residence by using a weighted distribution function based on the work trip distribution percentages. Note that we do not include cases where the home and work RSAs are the same because more movement in the simulated mobility patterns would facilitate the comparisons between considering and not considering the dynamics

Table 1

Regional Statistical Areas (RSAs) in LA County (Source: Los Angeles County Metropolitan Transportation Authority, 2010); (Note that RSAs 1–6 are located in Ventura County and thus not part of the study area.).

RSA	Area generally bounded by
7	Agoura Hills, Calabasas, Hidden Hills
8	Santa Clarita, Castaic
9	Lancaster, Gorman
10	Palmdale, Agua Dulce
11	Angeles National Forest
12	Woodland Hills, Sherman Oaks, Sepulveda, Porter Ranch
13	Burbank, Sun Valley, North Hollywood
14	San Fernando, Granada Hills, Sylmar, Tujunga
15	Malibu
16	Santa Monica, Bel Air, Palisades, Marina Del Rey
17	Westwood, Beverly Glen, Los Feliz, Hyde Park, Culver City
18	Westchester, Redondo Beach, Gardena, Inglewood
19	Torrance, Palos Verdes, Carson
20	Long Beach, Lakewood
21	Boyle Heights, Montebello, Compton, Willowbrook
22	Paramount, Hawaiian Gardens, Pico Rivera, La Habra Heights
23	Downtown Los Angeles, Exposition Park, MacArthur Park
24	Glendale, Echo Park, El Sereno
25	La Canada-Flintridge, Pasadena, Monterey Park, South El Monte, Duarte
26	Azusa, Glendora, Diamond Bar, Hacienda Heights
27	San Dimas, Pomona, Claremont

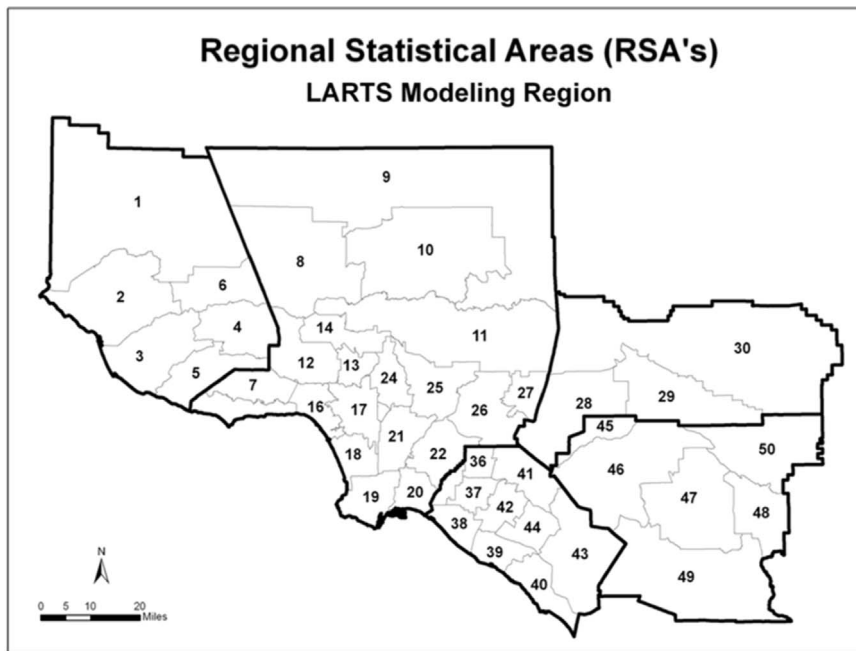


Fig. 3. Map of Regional Statistical Areas in LA County (Los Angeles County Metropolitan Transportation Authority, 2010).

of both human movement and air pollution. (3) The accurate work-residence locations within the selected RSAs are randomly distributed using a tool for generating random points in ESRI's ArcGIS software, until the randomly placed locations fall into the actual residential or work locations identified through a satellite view of Google Maps. Given that non-work activities are often conducted within an individual's space-time constraints that result from a set of locations of fixed daily activities, such as home and work (Kwan, 2004), non-work activity locations are generated using random points within a five-mile buffer of the home-work paths.

An example of a possible daily activity diary is presented in Table 2. The simulated data include each individual's trip information, such as latitude, longitude, activity start time, and activity type. The number of non-work activities conducted by each individual is randomly assigned within the range of 0 and 2. The duration of time at home that starts from midnight is randomly generated within the range of 360 and 540 min. Work duration is from 420 to 540 min, and non-work duration is from 30 to 120 min. The duration of time spent at home after work or non-work activities until midnight is designated as the rest of the day.

These simulated data are adequate for achieving the main research objective of this study—which is to highlight the potential for over- or underestimation of exposure levels and misleading findings about health risks when the dynamics of human movement and air pollution are not taken into account. One of the advantages of using simulated data is that researchers can generate a large dataset according to their needs. Another advantage is that the simulated data provide an opportunity for exploratory analysis, so that detailed analytical procedures can be developed and refined for implementation when real data

Table 2  
An example of a possible daily activity diary.

	Activity type	Latitude	Longitude	Start time	Duration (minutes)
Person 1	Home	34.04860	-118.24202	00:00	481
	Work	34.14957	-118.77580	08:56	535
	Non-work activity	34.08892	-118.34865	18:38	37
	Home	34.04860	-118.24202	19:27	272

are collected and become available with appropriate funding support.

### 2.3. Methods

#### 2.3.1. Estimation of hourly and daily ozone concentrations using cokriging

Cokriging can help to increase the spatiotemporal accuracy of estimations if a fine-scale temporal component is integrated into the modeling process. Cokriging is an extension of ordinary kriging that predicts values at unsampled locations using known (or measured) values. Since it uses secondary variables to improve the spatial accuracy of estimations of a primary variable, it can mitigate the spatial inaccuracy that ordinary kriging often suffers from due to the limited number of monitoring stations. It is especially useful for predicting ozone concentrations because it can consider secondary variables that contribute to ozone formation and dispersion. Ozone is a secondary pollutant that is formed in the atmosphere through the photochemical reactions of other pollutants, such as NOx and VOCs, and is more easily generated under high temperatures and low wind speeds (Chung, 1977, Gorai et al., 2015, Im et al., 2013, Ordóñez et al., 2005, Seinfeld and Pandis, 1998, Xu and Zhu, 1994). In this study, ozone is a primary variable in the cokriging analysis, while NOx and temperature are used as secondary variables. Because the temperature data have almost four times more samples than the ozone data have, spatial accuracy can be improved when compared to the accuracy of ordinary kriging estimates that are based solely on ozone data. To generate temporally more accurate prediction maps, cokriging can be iterated several times. We perform cokriging 24 times (once for each hour of the day) based on hourly ozone, hourly NOx, and hourly temperature data, so as to create an interpolated ozone map for each hour on February 23, 2014, the day for the monitoring site data.

In general terms, the method of cokriging is expressed as follows:

$$Z^{**} = \sum_{i=1}^n \lambda_i Z_i + \sum_{j=1}^m k_j u_j$$

where  $Z^{**}$  is the estimator,  $Z_i$  is the primary variable,  $u_j$  is the secondary variable,  $n$  and  $m$  are the number of samples for each of these two variables,  $\lambda_i$  is the weight for the primary variable, and  $k_j$  is the weight for the secondary variable. If some hourly ozone, NOx, and

temperature data are highly skewed, log transformation is performed to make them less skewed. Log transformation helps to reduce the root-mean-square error (RMSE). The RMSE—which is used to assess model accuracy—measures the differences between predicted values and observed values. The exponential variogram model is used because it minimizes the RMSE when compared to other variogram models, such as the spherical or Gaussian models. Model parameters, such as nugget, sill, and range, are optimized using cross-validation. These processes are repeated to make a daily average concentration map as well as each hourly map. The final outputs are 24 hourly ozone prediction maps and one daily map.

2.3.2. Comparisons of four types of personal exposure levels

To examine how personal or individual exposure levels may be different depending on whether human mobility and hourly variation of air pollution are considered, four types of personal exposure levels are estimated through (1) considering both human mobility and hourly pollution levels (hereafter, OO); (2) considering human mobility but not hourly pollution levels (using daily average pollution data) (hereafter, OX); (3) not considering human mobility (using residential locations) but hourly pollution levels (hereafter, XO); and (4) considering neither human mobility (using residential locations) nor hourly pollution (using daily average pollution) (hereafter, XX).

All hourly ozone prediction maps and the simulated daily movement data are combined to calculate personal mobility-based exposure estimates (i.e., in the OO case). The ozone concentration in a specific activity location is extracted from the ozone map at the corresponding hour. The total mobility-based exposure for an individual over the course of a day is calculated by summing up all exposure values. Next, residential locations are also combined with hourly ozone maps to calculate residence-based exposure estimates (i.e., in the XO case). Finally, human movement paths and residential locations are combined with a daily ozone map to calculate the estimates for the OX and XX cases, respectively. The paired sample t-tests are used to evaluate whether there are significant differences between these four types of estimates.

2.3.3. Investigation of the potential health effects of exposure to ozone using 3D geovisualization

To illustrate how spatiotemporally variable air pollution levels are,

how mobile people are, and how potential health effects can vary according to both of these dynamic patterns over the course of the day, we visualize some representative daily movement trajectories together with hourly ozone maps through 3D geovisualization (i.e., space is represented by the *x* and *y* axes, and time by the *z* axis), in which each hourly ozone map is stacked according to the corresponding hour. The segments of a daily movement trajectory passing through multiple prediction surfaces have different colors based on the severity of the potential health effects of the exposure level. Because daily movement data are minute-based and ozone concentration estimates are hour-based, exposure levels at a given hour are assumed to be temporally constant over the hour but spatially variable across the study area.

The GIS analyses and 3D geovisualization are performed with ESRI's ArcGIS software (ArcMap 10.2.1 and ArcScene 10.2.1), and the cokriging is conducted using the Geostatistical Analyst extension of ArcGIS. The paired sample t-tests are performed with the R statistical programming software. All graphs are created using R and GraphPad Prism 6.

3. Results

3.1. Spatiotemporal variability of ozone concentrations

Fig. 4 shows some of the hourly ozone maps created by cokriging (7 a.m., 8 a.m., 11 a.m., 5 p.m., 9 p.m., and 11 p.m.). These maps clearly reveal the spatial and temporal variations in ozone concentrations during the day in the study area. Much of the study area tends to have high ozone concentrations from 11 a.m. to 5 p.m. (0.041–0.075 ppm), while the levels are relatively low in the morning and at night. These temporal variations indicate that individuals may experience different exposure levels at different times of day even if they stay at the same location. In addition, although the ozone hot spots (areas with the highest ozone concentrations) change on an hourly basis, ozone levels in the southern west side tend to be continuously lower than those in the northern east side. This implies that individuals with different daily movement patterns may be exposed to different ozone concentrations even during the same period of time.

It is notable that the ozone hot spots are not in the urban areas with high population density and heavy traffic volume or high industrial occupancy. The spatial and temporal patterns of ozone concentrations

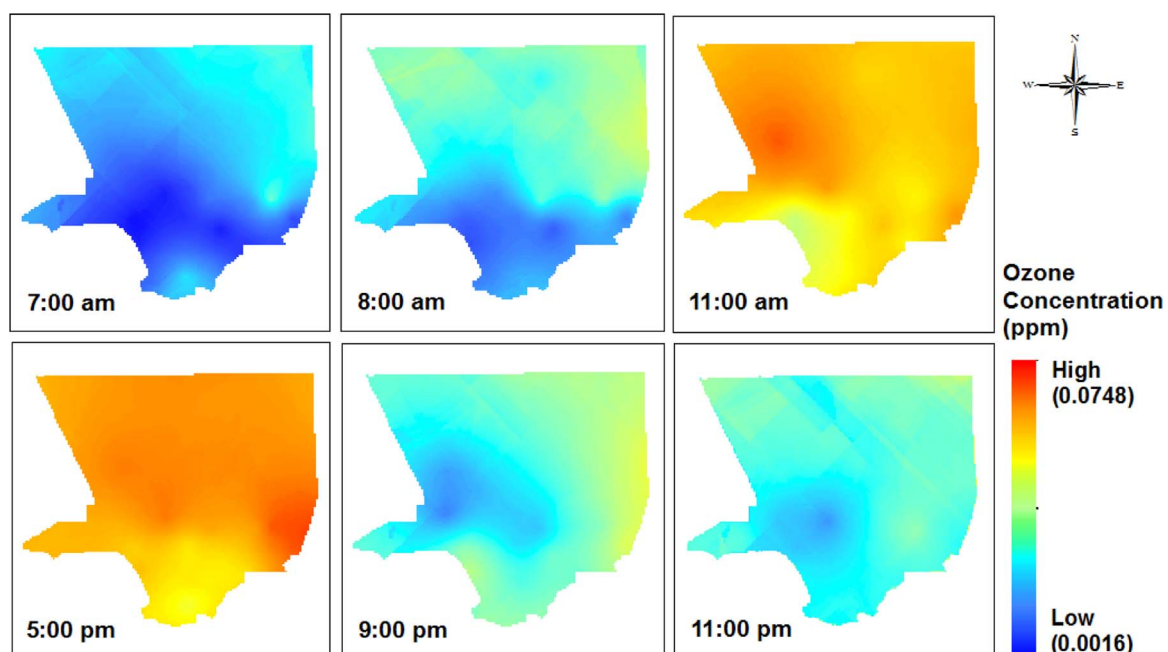


Fig. 4. Ozone concentrations at 7 a.m., 8 a.m., 11 a.m., 5 p.m., 9 p.m., and 11 p.m.

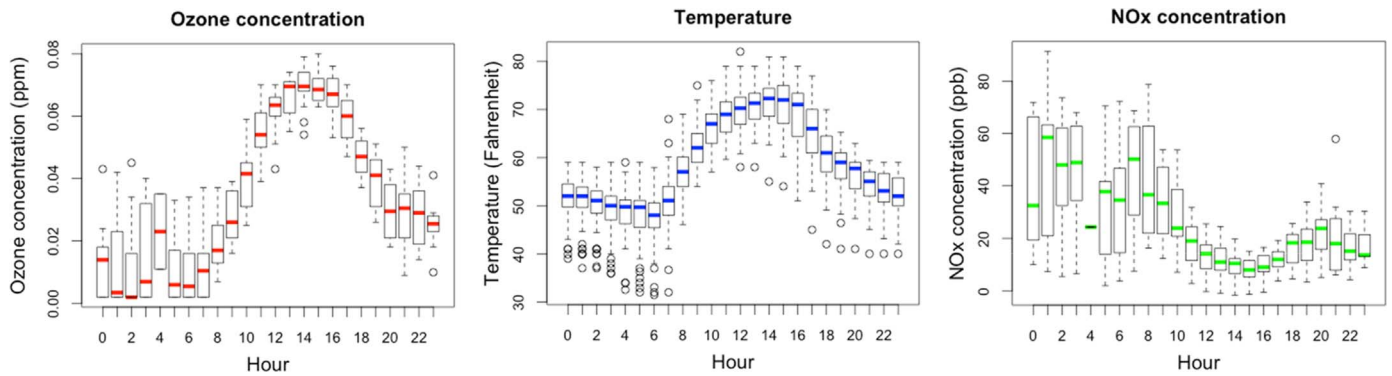


Fig. 5. Spatiotemporal variations in ozone concentrations, temperature, and NOx concentrations.

in the study area are opposite to those of NOx concentrations, which are directly influenced by emissions from vehicular traffic. Fig. 5 shows that the temporal patterns of ozone concentrations are positively correlated with those of temperatures but negatively associated with those of NOx. Some previous studies reported that ozone concentrations can be higher in rural than in urban areas (Duenas et al., 2005; Kalabokas et al., 2000; Klumpp et al., 2006; Wang et al., 2007). There are several reasons for this pattern. Generally, the highest ozone concentrations are observed downwind of urban areas rather than in the city itself, because the precursors of ozone move from hundreds to thousands of kilometers (Moussiopoulos and Sahm, 2000). In addition, rural areas tend to have more VOCs, which affect ozone formation (Bell and Ellis, 2004). The amount of biogenic VOC emissions prevalent in rural areas tends to be much more than that of the anthropogenic VOCs that are usually produced in urban areas. In addition, ozone can persist longer in rural areas, because nitric oxide concentrations that contribute to the destruction of ozone are lower in those areas (Klumpp et al., 2006).

3.2. Results of comparing four types of personal exposure estimates

The results of the paired sample t-tests that assess the differences among the four types of exposure estimates described earlier are presented in Table 3. Most of the pairs of estimates have very low p-values, indicating that the values of each type of estimates are significantly different from one another.

Each box plot in Fig. 6 displays the total exposure levels of the eighty individuals in the sample for each case. The lengths of the boxes of the OO (i.e., both mobility and hourly pollution estimates) and OX (i.e., mobility and daily estimates) cases are smaller than those of the boxes of the XO (i.e., residence and hourly estimates) and XX (i.e., residence and daily estimates) cases. This means that the difference in total exposure levels among the middle half of the samples (between the first and third quartiles) decreases when mobility is considered. It implies that the exposure levels among different individuals become more similar when people move to areas outside of their residential

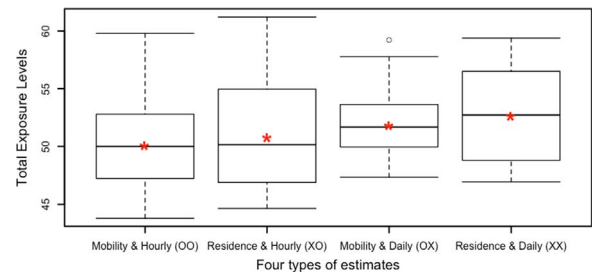


Fig. 6. Box plots of the total exposure levels of the 80 sampled individuals in the OO, XO, OX, and XX cases.

areas than when they spend the whole day within their residential areas. This means that, in this particular case, the diverse pollution levels people experience when they are mobile tend to reduce the exposure differences among individuals.

In addition, we can see in the box plots that the mean values of the four cases are different. The mean values are marked as red points in the plots. The mean value of the OO case is the smallest, and the mean value of the XX case is the largest. This indicates that the actual total exposure levels can be overestimated when residence-based data and temporally coarse data for air pollution (even daily data) are used.

Figs. 7 and 8 show the differences between two types of estimates for each individual in more detail. Fig. 7 includes hourly-daily comparisons (all \*O and \*X comparisons). The first plot indicates the differences between OO and XX of the 80 individuals. The differences are generated by subtracting XX from OO. The longer the bar is, the larger the difference between the two estimates. It is notable in these four graphs that many of the differences are negative numbers. This means that, regardless of using mobility- or residence-based data, the total exposure levels can be overestimated when daily average air pollution data are used rather than hourly data.

On the other hand, Fig. 8 includes mobility-residence comparisons (all O\* and X\* comparisons). Here, the differences look more variable than in the hourly-daily comparisons. There is much variation in both the magnitude and direction of the difference between mobility- and residence-based estimates. This finding suggests that actual exposure levels can be either over- or underestimated when residence-based data are used. Overestimation happens when people spend a significant amount of time in areas with better air quality than their residential areas, while underestimation happens when people spend a lot of waking time in more polluted areas than their residential areas. It is evident that a residential location does not fully represent an individual's true relevant geographic context in terms of air pollution exposure.

Table 3 Paired sample t-test results (significance of differences in the values of two different types of exposure estimates).

Pair of estimates	Mean of differences	p-value
OO & OX	1.745****	p < 0.0001
OO & XO	0.6923*	p=0.0188
OO & XX	2.572****	p < 0.0001
XO & OX	1.053***	p=0.0006
XO & XX	1.879****	p < 0.0001
OX & XX	0.8268**	p=0.0009

\* p < 0.05;  
 \*\*\* p < 0.001;  
 \*\*\*\* p < 0.0001

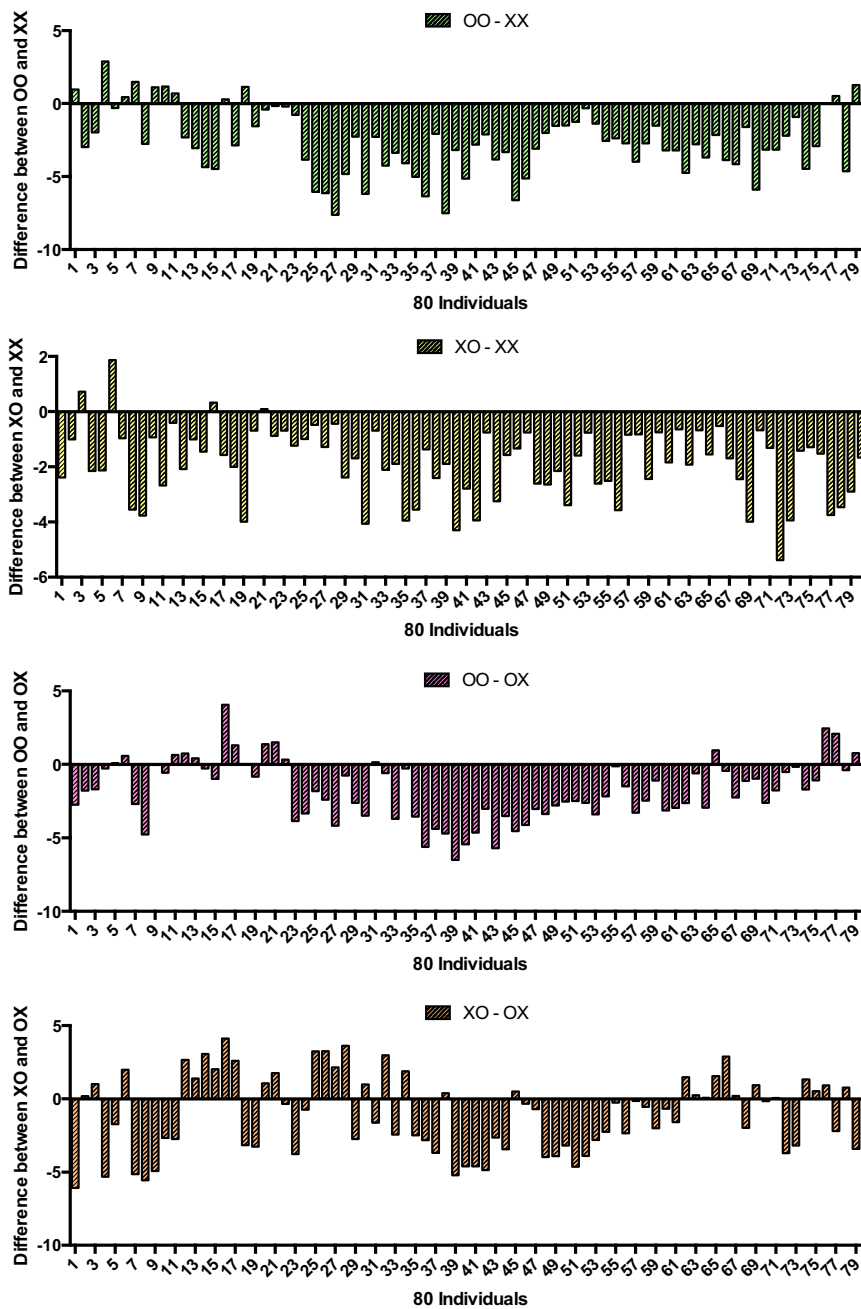


Fig. 7. Differences between hourly pollution-based and daily pollution-based exposure estimates.

### 3.3. 3D Geovisualization of spatiotemporally varying potential health effects

Three representative movement trajectories (Persons 24, 39, and 49) are geovisualized together with the 24 hourly interpolation maps of ozone concentrations in an interactive 3D scene in Fig. 9. The start and end points of a movement trajectory represent the residential location of an individual. The 3D scene shows how mobile humans interact with hourly changing ozone concentrations over the course of a day. We can see how these dynamic interactions lead to various personal exposure levels and potential health effects.

To better identify the potential health effects in the 3D scene, the segments of some of the movement trajectories are color-coded based on the severity of the potential health effects at a given exposure level. Ozone levels, potential health effects, and corresponding colors are presented in Table 4. Because the highest ozone concentration is

0.075 ppm in this study, the potential health impact of most ozone levels across the study area are within the ranges of “good” and “moderate” according to the US EPA’s Air Quality Index standard (in which more than 0.076 ppm ozone is considered “unhealthy”). However, a previous study demonstrated that elderly people are vulnerable even when they are exposed to a mere 0.030 ppm ozone (Simpson et al., 1997). In addition, exposure to 0.050 ppm can trigger mild respiratory symptoms in asthmatic children, such as coughing, breathing problems, and excessive phlegm production, and exposure to 0.065 ppm can cause respiratory symptoms to be more frequent for asthmatic children (Gielen et al., 1997).

As shown in Fig. 9, all three individuals tend to experience high levels of ozone concentration between 11 a.m. and 5 p.m. Even within this same period of time, however, individuals with different movement patterns experience different ozone levels and potential health effects depending on where they are and how long they stay there. Persons 24

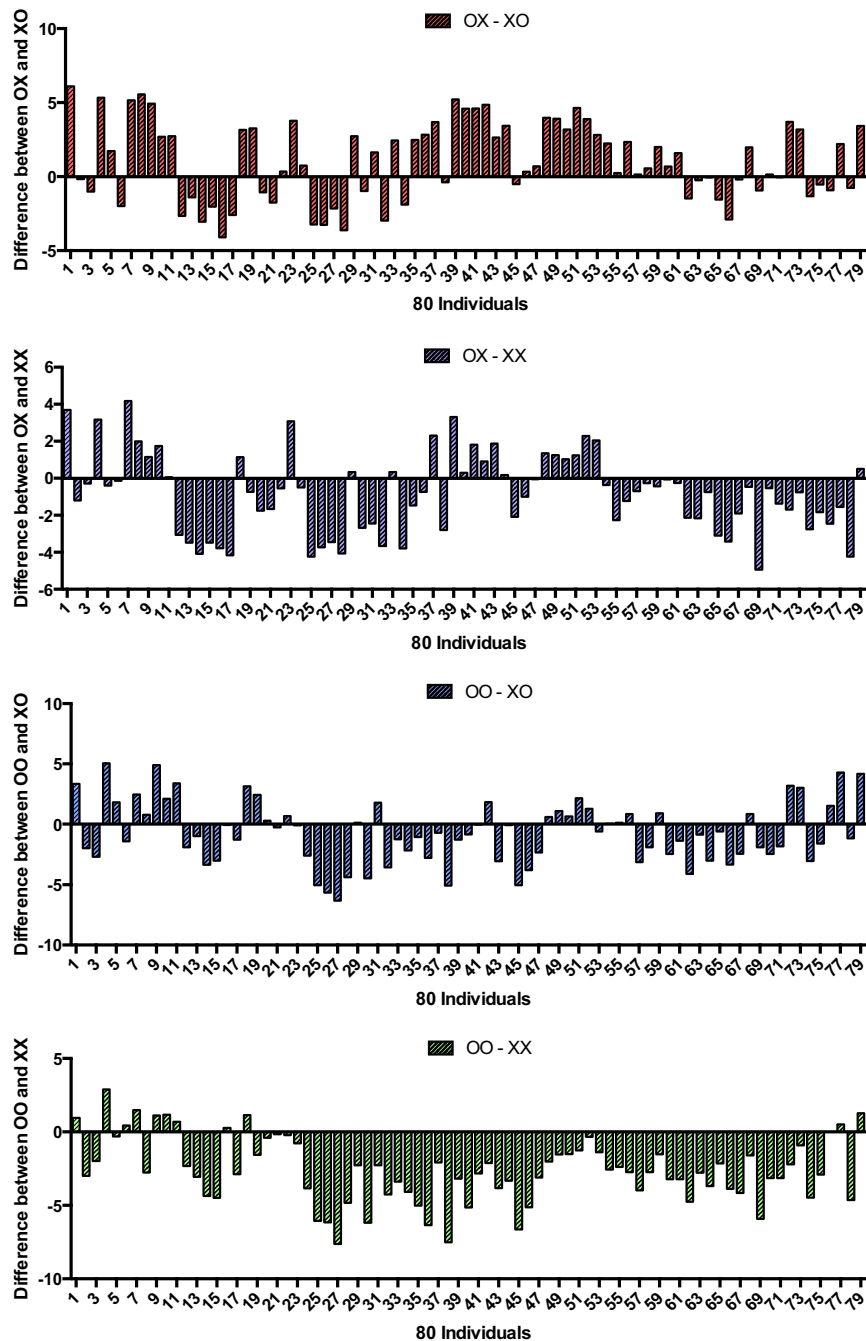


Fig. 8. Differences between mobility-based and residence-based exposure estimates.

and 49 have longer red-colored segments of the movement trajectories than Person 39, which means that they experience ozone concentrations over 0.065 ppm for a longer period of time than Person 39. This indicates that Person 39 is at relatively low health risk during the day compared to the other two people. Additionally, if Person 24 has asthma, he or she may experience increased symptoms for the longest time.

The reason for the differences in exposure levels and potential health risks among individuals is that each individual has a different “person-specific space-time context.” The person-specific dynamic space-time context is shaped by an individual’s daily activity locations and the routes used to move from one location to another. Research findings may be misleading due to the UGCoP if the different space-time contexts between individuals are not considered.

#### 4. Discussion and conclusions

This study contributes to the environmental health literature by demonstrating that considering both the spatiotemporal variability of air pollution and human daily movement patterns is vitally important for accurate exposure (or health risk) assessments. It also presents geospatial methods that enable researchers to take both of these variables into account. The results from the comparisons of the four types of exposure estimates suggest that exposure levels can be over- or underestimated due to the UGCoP if both of these variables are not considered simultaneously. These findings also call for more attention to the UGCoP, because it is a less recognized but important methodological problem that can significantly affect the accuracy of exposure assessment in environmental health research. The methods presented in this study highlight the potential impact of the UGCoP on research

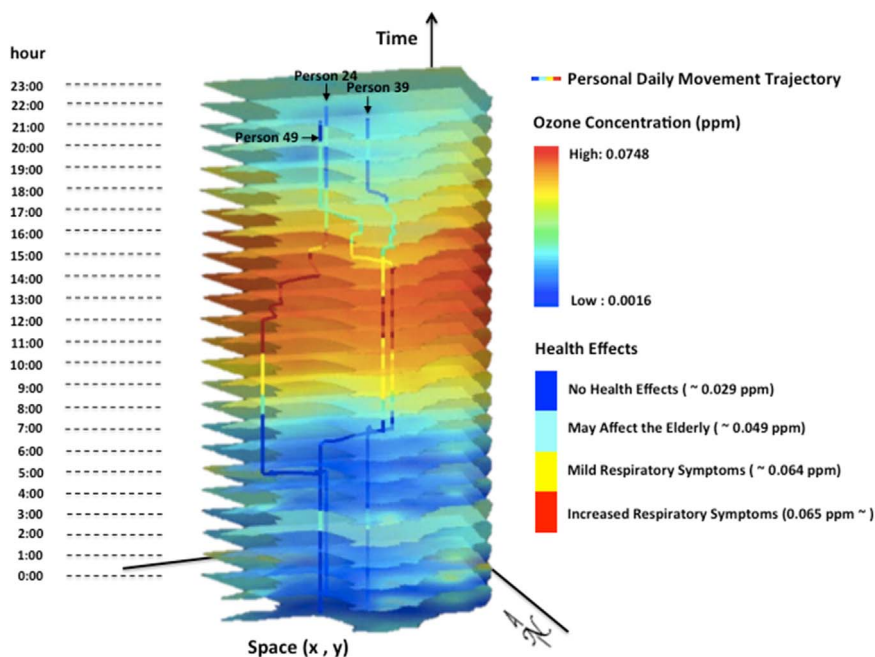


Fig. 9. 3D geovisualization of spatiotemporally changing personal exposure levels during a day and the potential effects on health. (For interpretation of the references to color in this figure legend, the reader is referred to the web version of this article.)

Table 4  
Ozone levels and the corresponding health effects.

Colors	Ozone concentrations (ppm)	Health effects (Gielen <i>et al.</i> 1997, Simpson <i>et al.</i> 1997)	Health effects based on Air Quality Index (US EPA)
Blue	0.000 – 0.029	No health effects are expected.	Good (No health effects are expected.)
	0.030 – 0.049	The elderly can be sensitive.	
Yellow	0.050 – 0.064	This level may trigger mild respiratory symptoms for asthmatic children.	Moderate (Unusually sensitive people may experience respiratory symptoms and should avoid prolonged outdoor activities.)
Red	0.065 – 0.075	This level may increase respiratory symptom frequency for asthmatic children.	

findings through considering both (1) the hourly variations in environmental or contextual factors (i.e., air pollution concentrations) rather than daily average data and (2) an individual's dynamic exposures at different times of day and in various activity locations as well as the relevant residential area. These methods allow for a more realistic evaluation of personal exposure levels and the potential health effects, because they enable a better approximation of the true geographic and temporal context in which an individual is exposed to air pollution.

This study clearly shows how advanced GIS, geospatial techniques, and 3D geovisualization can support empirical examination of the UGCoP and help to mitigate it. Guo *et al.* (2007) pointed out that it is challenging to visualize a complex dataset containing more than three dimensions (such as space, time, and one or more additional attributes) and to make the output easy to understand. However, recent advances in 3D GIS enable researchers to develop methods for visualizing and analyzing such complex data more effectively, which contributes significantly to expanding the frontier of environmental health research. The 3D geovisualization presented in this paper illustrates how the methods for considering both dynamic factors can help to capture the true relevant geographic and temporal contexts in which an individual is actually affected by air pollution and how such contexts vary among individuals. It also reveals that the complex spatiotemporal interactions between individuals and air pollutants create various person-specific space-time contexts, which in turn place different individuals at various levels of health risks. The visual examination of

the UGCoP calls for the development of dynamic conceptualizations of geographic contexts and sophisticated analytical approaches for mitigating contextual uncertainties in exposure assessment and environmental health research. Finally, the 3D geovisualization enables both researchers and the general public to more easily understand how personal daily exposure levels are spatially and temporally contingent. The general public, especially vulnerable groups such as women, children, or the elderly, can refer to this map to modify their daily behaviors. They can avoid going out or be more careful during peak hours of air pollution levels. It might also be possible to integrate the information on the potential health effects with mobile phone location data and/or voluntarily provided personal health data so that people could receive personalized warnings.

This study has several limitations that need to be addressed in future research. It does not consider the fact that indoor air quality may be different from outdoor air quality due to different pollution sources (e.g., heating or cooking fuel sources), although indoor air quality is partially influenced by outdoor air quality. Future research could expand upon these findings by using a reliable method to measure or estimate indoor air pollution levels. Although the present study assumes that each individual uses the same travel mode during a day, future studies could improve the accuracy of the results by considering the effects of different travel modes (e.g., commuting by car versus riding a bicycle) on the inhalation rates. Further, due to fewer monitoring sites at non-peak hours than at peak hours, the estimation of ozone concentrations at non-peak hours still have non-negligible errors, although these estimates can be improved by using secondary variables in cokriging analysis. In future studies, air dispersion models that are less affected by the number of monitoring sites—that use emission, meteorological, and topographic data, which address the dispersion of air pollutants in the atmosphere—can be used to improve the accuracy of air pollution estimates. Finally, future research can use movement tracking data (e.g., GPS data) collected from real human subjects in order to assess actual exposure levels. The methods used in this study can readily be applied to such high-resolution movement datasets. If these datasets also include individuals' socio-economic and demographic information (e.g., race, gender, income, education, and class), the method can be used to more accurately examine the relationships between air pollution exposure and indivi-

duals' socioeconomic characteristics. The findings of such kind of research would provide useful answers to many interesting questions, such as: Which social group is at the highest health risk associated with exposure to air pollution? To what extent do different social groups experience unequal exposure levels in their daily lives? Being able to identify the population group(s) with the highest health risk based on more accurate individual-level data will lead to more effective intervention measures that mitigate social inequalities associated with various environmental risk factors.

## References

- Bell, M., Ellis, H., 2004. Sensitivity analysis of tropospheric ozone to modified biogenic emissions for the Mid-Atlantic region. *Atmos. Environ.* 38 (13), 1879–1889.
- Buonanno, G., Stabile, L., Morawska, L., 2014. Personal exposure to ultrafine particles: the influence of time-activity patterns. *Sci. Total Environ.* 468–469, 903–907.
- Bureau of the Census, 2015. *County business patterns 2013*. US Department of Commerce, Bureau of the Census Washington, DC.
- Buzzelli, M., Jerrett, M., 2007. Geographies of susceptibility and exposure in the city: environmental inequity of traffic-related air pollution in Toronto. *Can. J. Reg. Sci.* 2, 195–210.
- Chen, X., Kwan, M.-P., 2015. Contextual uncertainties, human mobility, and perceived food environment: the uncertain geographic context problem in food access research. *Am. J. Public Health* 105 (9), 1734–1737.
- Chum, A., O'Campo, P., 2013. Contextual determinants of cardiovascular diseases: overcoming the residential trap by accounting for non-residential context and duration of exposure. *Health Place* 24, 73–79.
- Chung, Y.S., 1977. Ground-level ozone and regional transport of air pollutants. *J. Appl. Meteorol.* 16 (11), 1127–1136.
- Crawford, T.W., et al., 2014. Conceptualizing and comparing neighborhood and activity space measures for food environment research. *Health Place* 30, 215–225.
- Dons, E., et al., 2011. Impact of time-activity patterns on personal exposure to black carbon. *Atmos. Environ.* 45 (21), 3594–3602.
- Duenas, C., et al., 2005. Stochastic model to forecast ground-level ozone concentration at urban and rural areas. *Chemosphere* 61, 1379–1389.
- Fang, T.B., Lu, Y., 2012. Personal real-time air pollution exposure assessment methods promoted by information technological advances. *Ann. GIS* 18 (4), 279–288.
- Gielen, M.H., et al., 1997. Acute effects of summer air pollution on respiratory health of asthmatic children. *Am. J. Respir. Crit. Care Med.* 155 (6), 2105–2108.
- Gorai, A.K., et al., 2015. Influence of local meteorology and NO<sub>2</sub> conditions on ground-level ozone concentrations in the eastern part of Texas. (USA) *Air Qual. Atmos. Health* 8 (1), 81–96.
- Gray, S.C., Edwards, S.E., Miranda, M.L., 2013. Race, socioeconomic status, and air pollution exposure in North Carolina. *Environ. Res.* 126, 152–158.
- Guo, D., Liao, K., Morgan, M., 2007. Visualizing patterns in a global terrorism incident database. *Environ. Plan. B: Plan. Des.* 34, 767–784.
- Hägerstrand, T., 1970. What about people in regional science? *Papers of Regional Science Association* 24, 7–21.
- Hernandez, M., Collins, T.W., Grineski, S.E., 2015. Immigration, mobility, and environmental injustice: a comparative study of Hispanic people's residential decision-making and exposure to hazardous air pollutants in Greater Houston. (Texas) *Geoforum* 60, 83–94.
- Im, U., et al., 2013. Analysis of surface ozone and nitrogen oxides at urban, semi-rural and rural sites in Istanbul, Turkey. *Sci. Total Environ.* 443, 920–931.
- Jerrett, M., et al., 2001. A GIS-environmental justice analysis of particulate air pollution in Hamilton. (Canada) *Environ. Plan. A* 33 (6), 955–973.
- Kalabokas, P.D., et al., 2000. Mediterranean rural ozone characteristics around the urban area of Athens. *Atmos. Environ.* 34, 5199–5208.
- Klumpp, A., et al., 2006. Ozone pollution and ozone biomonitoring in European cities. Part I: ozone concentrations and cumulative exposure indices at urban and suburban sites. *Atmos. Environ.* 40, 7963–7974.
- Kwan, M.-P., 2004. GIS methods in time-geographic research: geocomputation and geovisualization of human activity patterns. *Geogr. Ann.: B* 86 (4), 267–280.
- Kwan, M.-P., 2009. From place-based to people-based exposure measures. *Soc. Sci. Med.* 69 (9), 1311–1313.
- Kwan, M.-P., 2012a. The uncertain geographic context problem. *Ann. Assoc. Am. Geogr.* 102 (5), 958–968.
- Kwan, M.-P., 2012b. How GIS can help address the uncertain geographic context problem in social science research. *Ann. GIS* 18 (4), 245–255.
- Kwan, M.-P., Schuurman, N., 2004. Issues of privacy protection and analysis of public health data. *Cartographica* 39 (2), 1–4.
- Kwan, M.-P., Casas, I., Schmitz, B.C., 2004. Protection of geoprivacy and accuracy of spatial information: how effective are geographical masks? *Cartographica* 39 (2), 15–28.
- Kwan, M.-P., Liu, D., Vogliano, J., 2015. Assessing dynamic exposure to air pollution. In: Kwan, M.-P., Richardson, D., Wang, D., Zhou, C. (Eds.), *Space-Time Integration in Geography and GIScience: Research Frontiers in the US and China*. Springer, Dordrecht, 283–300.
- Liao, Y., Intille, S.S., Dunton, G.F., 2014. Using ecological momentary assessment to understand where and with whom adults' physical and sedentary activity occur. *Int. J. Behav. Med.* 22, 51–61.
- Los Angeles County Metropolitan Transportation Authority, 2010. *congestion management program (2010)*. Author, Los Angeles, CA.
- Lu, Y., Fang, T., 2015. Examining personal air pollution exposure, intake, and health danger zone using time geography and 3D geovisualization. *ISPRS Int. J. Geo-Inf.* 4, 32–46.
- Moussiopoulos, N., Sahn, P., 2000. The OFIS model: an efficient tool for assessing ozone exposure and evaluating air pollution abatement strategies. *Int. J. Environ. Pollut.* 14, 597–606.
- de Nazelle, A., et al., 2013. Improving estimates of air pollution exposure through ubiquitous sensing technologies. *Environ. Pollut.* 176, 92–99.
- Nyhan, M., et al., 2016. "Exposure track"—the impact of mobile-device-based mobility patterns on quantifying population exposure to air pollution. *Environ. Sci. Technol.* 50 (17), 9671–9681.
- Ordóñez, C., et al., 2005. Changes of daily surface ozone maxima in Switzerland in all seasons from 1992 to 2002 and discussion of summer 2003. *Atmos. Chem. Phys.* 5, 1187–1203.
- Park, Y.M., Kim, Y., 2014. A spatially filtered multilevel model to account for spatial dependency: application to self-rated health status in South Korea. *Int. J. Health Geogr.* 13, 6.
- Pilla, F., Broderick, B., 2015. A GIS model for personal exposure to PM10 for Dublin commuters. *Sustain. Cities Soc.* 15, 1–10.
- Robinson, A.I., Oreskovic, N.M., 2013. Comparing self-identified and census-defined neighborhoods among adolescents using GPS and accelerometer. *Int. J. Health Geogr.* 12, 57.
- Ryan, P.H., et al., 2015. A field application of a personal sensor for ultrafine particle exposure in children. *Sci. Total Environ.* 508, 366–373.
- Seinfeld, J.H., Pandis, S.N., 1998. *Atmospheric Chemistry and Physics from Air Pollution to Climate Change*. John Wiley and Sons, New York, NY.
- Setton, E., et al., 2011. The impact of daily mobility on exposure to traffic-related air pollution and health effect estimates. *J. Expo. Sci. Environ. Epidemiol.* 21, 42–48.
- Setton, E., Keller, C.P., Cloutier-Fisher, D., Hystad, P.W., 2008. Spatial variations in estimated chronic exposure to traffic-related air pollution in working populations: a simulation. *Int. J. Health Geogr.* 7, 39.
- Simpson, R.W., et al., 1997. Association between outdoor air pollution and daily mortality in Brisbane, Australia. *Arch. Environ. Health* 52 (6), 442–454.
- Steinle, S., et al., 2015. Personal exposure monitoring of PM2.5 in indoor and outdoor microenvironments. *Sci. Total Environ.* 508, 383–394.
- Steinle, S., Reis, S., Sabel, C.E., 2013. Quantifying human exposure to air pollution—Moving from static monitoring to spatio-temporally resolved personal exposure assessment. *Sci. Total Environ.* 443, 184–193.
- US EPA., 1993. *Automobiles and Ozone (EPA 400-F-92-006)*. Environmental Protection Agency Office of Mobile Sources, Washington, DC: U.S.
- Wang, X., et al., 2007. Ground-level ozone in China: distribution and effects on crop yields. *Environ. Pollut.* 147, 394–400.
- Weaver, R., 2014. Contextual influences on political behavior in cities: toward urban electoral geography. *Geogr. Compass* 8 (12), 874–891.
- Xu, J., Zhu, Y., 1994. Some characteristics of ozone concentrations and their relations with meteorological factors in Shanghai. *Atmos. Environ.* 28 (20), 3387–3392.
- Yoo, E., et al., 2015. Geospatial estimation of individual exposure to air pollutants: moving from static monitoring to activity-based dynamic exposure assessment. *Ann. Assoc. Am. Geogr.* 105 (5), 915–926.
- Zhou, J., et al., 2011. Health risk assessment of personal inhalation exposure to volatile organic compounds in Tianjin, China. *Sci. Total Environ.* 409 (3), 452–459.